Available online at www.sciencedirect.com
SCIENCE DIRECT®
Pergamon
Neuropharmacology 45 (2003) 220–230
NEURO PHARMACOLOGY
www.elsevier.com/locate/neuropharm

Distribution of ORL-1 receptor binding and receptor-activated G-proteins in rat forebrain and their experimental localization in anterior cingulate cortex

Laura J. Sim-Selley [a,*], Leslie J. Vogt [b,c], Steven R. Childers [b], Brent A. Vogt [b,c]

[a] *Department of Pharmacology and Toxicology and Institute for Drug and Alcohol Studies, Virginia Commonwealth University Medical College of Virginia, Richmond, VA 23298, USA*

[b] *Department of Physiology and Pharmacology and Center for Investigative Neuroscience, Wake Forest University School of Medicine, Winston–Salem, NC 27157, USA*

[c] *Cingulum NeuroSciences Institute, Syracuse, NY 13210, USA*

Received 3 February 2003; received in revised form 18 March 2003; accepted 1 April 2003

Abstract

Opioid receptor-like (ORL-1) receptors and ORL-1-activated G-proteins are found in high levels in the forebrain, particularly cingulate cortex, an area involved in processing of nociceptive stimuli. [^{3}H]nociceptin/orphanin FQ (N/OFQ) and N/OFQ-stimulated [^{35}S]GTPγS autoradiography in rat brain were used to localize ORL-1 receptors and activated G-proteins, respectively. N/OFQ binding and activated G-proteins were highest in anterior cingulate, agranular insula, piriform, perirhinal and entorhinal cortices; midline and intralaminar thalamic nuclei; and subnuclei of the amygdala and hippocampus. In anterior cingulate area 24, [^{3}H]N/OFQ and N/OFQ-stimulated [^{35}S]GTPγS binding were highest in layers V and VI. The cellular localization of ORL-1 receptors and activated G-proteins in area 24 was examined using two strategies: ibotenic acid injection into the cortex or undercut lesions to remove afferent axons, followed by autoradiography. Ibotenic acid lesions that destroyed neurons in the anterior cingulate cortex decreased [^{3}H]N/OFQ binding by 75–80% and reduced N/OFQ-stimulated [^{35}S]GTPγS binding to basal levels seen in the absence of agonist. Deafferentation lesions increased [^{3}H]N/OFQ binding by 40–50%, with no significant change in N/OFQ-stimulated [^{35}S]GTPγS binding. These data demonstrate that ORL-1 receptors in layer V of anterior cingulate cortex are located on somatodendritic elements and that deafferentation increases ORL-1 receptor binding.

Keywords: Nociceptin; Orphanin FQ; Opioid receptor; Nociception

Abbreviations: ACC, Anterior cingulate cortex; ACo, Cortical nucleus of the amygdala; AHi, Amygdalohippocampal area; AI, Agranular insular cortex; AO, Anterior olfactory nucleus; Arc, Arcuate nucleus; AV, Anteroventral thalamic nucleus; BMA, Basomedial amygdaloid nucleus; Ce, Central amygdaloid nucleus; CG, Central gray; Cl, Claustrum; CM, Central medial thalamic nucleus; DI, Dysgranular insular cortex; DG, Dentate gyrus; DLG, Dorsal lateral geniculate nucleus; En, Endopiriform nucleus; ENT, Entorhinal cortex; Fr, Frontal cortex; GI, Granular insular cortex; HIP, Hippocampus; HL, Hindlimb area; IAM, Interanteromedial thalamic nucleus; LA, Lateral amygdaloid nucleus; LD, Laterodorsal thalamic nucleus; LO, Lateral orbital cortex; LP, Lateral posterior thalamic nucleus; LS, Lateral septal nucleus; MG, Medial geniculate nucleus; MM, Medial mammillary nucleus; MS, Medial septal nucleus; NAc, Nucleus accumbens; PaS, Parasubiculum; PC, Paracentral thalamic nucleus; PF, Parafascicular thalamic nucleus; PIR, Piriform cortex; PRh, Perirhinal cortex; PrS, Presubiculum; Po, Posterior thalamic nuclear group; PV, Paraventricular thalamic nucleus; Rt, Reticular thalamic nucleus; S, Subiculum; SC, Superior colliculus; SCh, Suprachiasmatic nucleus; SG, Supragenicular thalamic nucleus; SO, Supraoptic nucleus; SuG, Superficial gray layer of the superior colliculus; SuM, Supramammillary nucleus; Te, Temporal cortex; TT, Tenia tecta; Tu, Olfactory tubercle; VL, Ventrolateral thalamic nucleus; VLG, Ventral lateral geniculate nucleus; VLO, Ventral lateral orbital cortex; VMH, Ventromedial hypothalamic nucleus.

* Corresponding author. Tel.: +1-804-827-0464; fax:+1-804-828-1532.

E-mail address: ljsimsel@hsc.vcu.edu (L.J. Sim-Selley).

0028-3908/03/$ - see front matter © 2003 Elsevier Science Ltd. All rights reserved.
doi:10.1016/S0028-3908(03)00155-2

1. Introduction

The opioid receptor-like (ORL-1) receptor exhibits structural homology to mu, delta and kappa opioid receptors, but does not bind classic opioid receptor ligands (Bunzow et al., 1994; Fukuda et al., 1994; Mollereau et al., 1994; Wang et al., 1994; Wick et al., 1994; Lachowicz et al., 1995). ORL-1 receptors bind an endogenous peptide, nociceptin or orphanin FQ (N/OFQ), which is structurally similar to opioid peptides, but lacks the amino terminal tyrosine common to opioids (Meunier et al., 1995; Reinscheid et al., 1995). N/OFQ produces the same intracellular effects as opioids, including inhibition of adenylyl cyclase (Meunier et al., 1995; Reinscheid et al., 1995), increased K^+ conductance (Matthes et al., 1996; Vaughn and Christie, 1996) and decreased Ca^{2+} conductance (Knoflach et al., 1996). These effects are consistent with activation of inhibitory G-proteins of the G_i/G_o family.

N/OFQ binding sites (Florin et al., 1997; Neal et al., 1999b) and receptor-activated G-proteins (Sim et al., 1996), as well as N/OFQ peptide and pre-pro N/OFQ mRNA (Neal et al., 1999a), are found in moderate to high levels throughout the cerebral cortex. Autoradiographic analysis of ^{125}I–[^{14}Tyr]–OFQ binding has revealed the highest cortical labeling in the cingulate cortex (Neal et al., 1999b). ORL-1 receptor immunoreactivity exhibits a similar cortical distribution (Anton et al., 1996); however, the precise immunocytochemical localization of ORL-1 receptors is unclear due to questions concerning the specificity of the ORL-1 antibodies (Evans, 1999). Although these studies provide data regarding the anatomical distribution of various components of the ORL-1 system, the relationship between ORL-1 receptor binding sites and receptor-mediated G-protein activity has not been established. Furthermore, these studies have not addressed the cellular localization of ORL-1 receptors and activated G-proteins in the cortex.

ORL-1 has been implicated in a variety of functions, including motor, sensory, memory, stress and autonomic effects (Meunier, 1997; Neal et al., 1999a). One of the first reported actions of N/OFQ was hyperalgesia following intracerebroventricular (i.c.v.) injection (Meunier et al., 1995; Reinscheid et al., 1995). Subsequent studies have shown that although N/OFQ produces hyperalgesia when administered i.c.v., intrathecal N/OFQ administration produces analgesia (King et al., 1997; Hao et al., 1998). Furthermore, i.c.v. N/OFQ antagonizes morphine-induced analgesia (Grisel et al., 1996; Mogil et al., 1996; Tian et al., 1997; Zhu et al., 1997), suggesting that supraspinal ORL-1 receptors modulate the opioid system. Recent studies indicate that N/OFQ in the cingulate cortex may be particularly important in chronic pain states. Nerve ligation or carageen-induced inflammation resulted in increased levels of N/OFQ-like immunoreactivity in the cingulate cortex (Rosen et al., 2000). The anterior cingulate cortex (ACC) contains nociceptive neurons (Sikes and Vogt, 1992) and is activated in the human brain during noxious stimulation (Jones et al., 1991; Casey et al., 1994; Coghill et al., 1994; Vogt et al., 1996). This data, together with anatomical data showing high levels of ORL-receptors, suggests that ACC may be an important region in the nociceptive action of N/OFQ.

The present studies were performed to elucidate the relationship between ORL-1 binding sites and receptor-activated G-proteins in the forebrain, with emphasis on ORL-1 in the ACC. Furthermore, the cellular localization of ORL-1 receptors and activated G-proteins in the ACC was determined using lesion strategies that have previously been applied to receptor localization in this region (Vogt et al., 1995).

2. Methods

2.1. Materials

Male Long Evans rats (350–400 g) were purchased from Harlan Laboratories (Indianapolis, IN). The animals were maintained in an AAALAC approved facility and all experimental procedures were approved by the Wake Forest University School of Medicine Animal Use and Care Committee. [^{35}S]GTPγS (1250 Ci/mmol) was purchased from New England Nuclear Corp. (Boston, MA). [^{3}H]N/OFQ (30 Ci/mmol) was purchased from Phoenix Pharmaceuticals, Inc. GDP was obtained from Sigma Chemical Co. (St. Louis, MO). Reflections® autoradiography film was purchased from New England Nuclear Corp. (Boston, MA) and Hyperfilm βmax was obtained from Amersham Life Sciences (Arlington Heights, IL). The N/OFQ peptide was synthesized in the Protein Core Laboratory of the Cancer Center at Wake Forest University. All other reagent grade chemicals were obtained from Sigma Chemical Co. or Fisher.

2.2. Lesions

Rats were anesthetized with Chloropent (0.3 ml/100 g body weight i.p.), then received either ibotenic acid or deafferentation lesion as previously described (Vogt et al., 1995). Stereotaxic coordinates (Paxinos and Watson, 1986) were used to guide placement of injections and scalpel blade cuts, but the extent of each lesion was determined in thionin stained sections. Excitotoxin lesions were made by placing two injections of ibotenic acid (3–3.5 μl per injection of 10 μg ibotenic acid/μl 0.9% saline) unilaterally into area 24 (stereotaxic coordinates: +1.0 and +0.4 mm anterior to bregma; 0.5 mm lateral to the midline; 2.4 mm ventral to the cortical surface; *N*=7). Unilateral undercut lesions were made by

passing a scalpel blade 1.6 mm lateral to the midline, 4.5 mm ventral to the cortical surface of the brain extending from 1.7 mm anterior to bregma to 1.0 mm posterior to bregma (*N*=6). Coronal knife cuts were made at the rostral and caudal extents of the knife cut. After a two week survival period, animals were sacrificed by decapitation, and brains were removed and frozen in isopentane at −30° C. Brains from four animals that did not receive lesions were also collected. Coronal sections through the rostral–caudal extent of the cingulate cortex were cut on a cryostat maintained at −20° C, mounted directly onto gelatin subbed slides and collected in a humid chamber. In each case, a series of slides with triplicate sections (12 slides for undercut, 8 slides for excitotoxin) was cut at 20 μm for autoradiography followed by a slide containing 3 sections cut at 50 μm for thionin staining. Slides were desiccated at 4° C overnight, then stored desiccated at −80° C until use.

2.3. [^{3}H]N/OFQ autoradiography

Slides were stored at −20° C for 24 h prior to assay. On the day of the assay, slides were brought to room temperature with a cool air dryer, then processed as follows. Slides were equilibrated in 50 mM Tris buffer containing 3 mM $MgCl_2$ and 0.2 mM EGTA, pH 7.6 (TME buffer) with protease inhibitors (10 μl/ml of a solution containing 0.2 mg/ml each of bestatin, leupeptin, pepstatin A and aprotinin) for 15 min at 25° C. Slides were rinsed in TME buffer at 25° C for 10 min, and incubated in 0.5 nM [^{3}H]N/OFQ in TME buffer with 0.5% BSA for 1 h at 25° C. Nonspecific binding was measured in the presence of 10 μM N/OFQ. Slides were rinsed 3 times in 50 mM Tris buffer (pH 7.6) on ice, and once for 30 s in deionized H_2O on ice. Slides were dried completely and exposed to Hyperfilm for 8 weeks, along with a [^{3}H] microscale in each cassette for quantification. A subset of slides was also processed for coverslip autoradiography as previously described (Vogt et al., 1992). Acid cleaned coverslips were dipped in NTB-2 emulsion and completely dried, then apposed to slides that were stored at −20° C for 10 weeks. Slides were developed in Kodak D-19, fixed in Kodak rapid fix without hardener and counterstained with thionin.

2.4. [^{35}S]GTPγS autoradiography

Slides were removed from the freezer and brought to room temperature under a stream of cool air. Sections were equilibrated in 50 mM Tris buffer (pH 7.4) containing 3 mM $MgCl_2$, 0.2 mM EGTA and 100 mM NaCl (TME/NaCl buffer) for 10 min at 25° C. Sections were incubated in TME/NaCl buffer containing 2 mM GDP and protease inhibitors (10 μl/ml of a solution containing 0.2 mg/ml each of bestatin, leupeptin, pepstatin A and aprotinin) for 15 min at 25° C. Sections were then incubated in 3 μM N/OFQ, 0.04 nM [^{35}S]GTPγS and 2 mM GDP in TME/NaCl buffer at 25° C for 2 h. Basal binding was assessed in the absence of agonist. Slides were rinsed twice for 2 min each in 50 mM Tris buffer (pH 7.4) at 4° C, then for 30 s in deionized H_2O at 4° C. Slides were dried overnight and exposed to Reflections® film for 48 h. Each cassette contained a [^{14}C] microscale for densitometric analysis. A subset of slides was also processed for coverslip autoradiography as described above.

2.5. Nomenclature

The areal and laminar distribution of [^{3}H]N/OFQ and N/OFQ-stimulated [^{35}S]GTPγS binding in the cortex was verified by microscopic examination of thionin-stained sections and sections processed for coverslip autoradiography. Nomenclature is from (Paxinos and Watson, 1986) and (Zilles, 1985). The cingulate cortex is parcellated according to Vogt and Peters (1981).

2.6. Data analysis

Thionin-stained sections were examined to verify the extent and localization of the lesions. For each lesion, certain criteria were required for brains to be included in the densitometric analysis. For ibotenic acid lesions, only brains that had complete neurodegeneration in the measurement field were used for analysis; small lesions that did not meet this criterion were not used for subsequent analysis. For deafferentation studies, brains in which knife cuts damaged the tissue in the cingulate cortex were not used for analysis. No evidence of stroke was seen following lesion, which has previously been demonstrated using electron microscopy (Vogt, 1993). Four brains met the criterion for ibotenic acid lesion and six brains met the criterion for undercut lesion. Films were digitized with a Sony XC-77 video camera and analyzed using the NIH Image program for Macintosh computers. In all cases, measurements were made using a standard rectangular area that was placed over layer V of areas 24a and 24b. The same standard rectangle was used to measure binding in all cases. For agonist-stimulated [^{35}S]GTPγS binding, [^{14}C] values were corrected for [^{35}S] based upon incorporation of [^{35}S] into sections of frozen brain paste. Agonist stimulated [^{35}S]GTPγS binding and [^{3}H]N/OFQ binding are expressed in fmol/mg. Data are reported as mean values ± standard error (S.E.) of triplicate sections of brains from 4–6 animals. Statistical significance of the data was determined by the non-paired two tailed Student's *t*-test using JMP (SAS Institute, Cary, NC). Correlation analyses were performed by linear regression with JMP.

3. Results

3.1. [^{3}H]N/OFQ and N/OFQ-stimulated [^{35}S]GTPγS binding in forebrain

Moderate to high levels of ORL-1 receptors and activated G-proteins were found in many regions of the telencephalon and diencephalon. [^{3}H]N/OFQ binding and N/OFQ-stimulated [^{35}S]GTPγS binding exhibited the same neuroanatomical distribution and appeared to be similar in magnitude in most regions. Eight forebrain regions with particularly high levels of [^{3}H]N/OFQ and N/OFQ-stimulated [^{35}S]GTPγS binding were analyzed densitometrically and the results are presented in Table 1. Statistical analysis showed that the ACC, entorhinal (ENT) and anterior piriform (PIR) cortices shared a high and similar level of binding. The superior colliculus (SC), ventromedial hypothalamic nucleus (VMH), central medial thalamic nucleus (CM) and CA2/3 regions of the hippocampus had similar levels of [^{3}H]N/OFQ binding that were lower than the cortical areas. Finally, the lateral nucleus of the amygdala was intermediate between these two levels of binding and did not differ from either category. Another way of visualizing these findings is to plot [^{3}H]N/OFQ binding against N/OFQ-stimulated [^{35}S]GTPγS binding. Fig. 1 illustrates the close relationships between the three cortical (ACC, PIR, ENT) and three subcortical (CM, SC, VMH) regions. The linear regression of these points has a high r coefficient (r=0.94) and confirms that regions with high levels of ORL-1 receptor binding contain high levels of ORL-1-activated G-proteins.

Fig. 2a–d show representative autoradiograms of [^{3}H]N/OFQ and N/OFQ-stimulated [^{35}S]GTPγS binding throughout the rostral–caudal extent of the forebrain. The analysis of different forebrain regions is important

Table 1
Distribution of N/OFQ receptor binding and activated G-proteins

Region	[^{3}H]ORL	[^{35}S]GTPγS
Anterior cingulate cortex	85±10	0.46±0.048
Entorhinal cortex	75±1.9	0.38±0.023
Anterior piriform cortex	70±2.0	0.46±0.028
Amygdala: LA	61±2.4	0.32±0.041
Superior colliculus	46±1.7	0.22±0.013
Hypothalamus: VM	43±1.1	0.25±0.062
Medial thalamus: CM	42±3.3	0.19±0.037
Hippocampus: CA2/3	30±1.6	0.19±0.028

The results of densitometric analysis of [^{3}H]N/OFQ and N/OFQ-stimulated [^{35}S]GTPγS binding in eight forebrain regions containing high levels of binding are shown. The following areas were analyzed densitometrically: area 24a at the level of the genu of the corpus callosum; layers V and VI of the entorhinal and piriform cortices; superficial layer of the superior colliculus; and hippocampus CA 2/3 molecular layer. Values are expressed in fmol/mg and are the results from triplicate sections from 4 control animals.

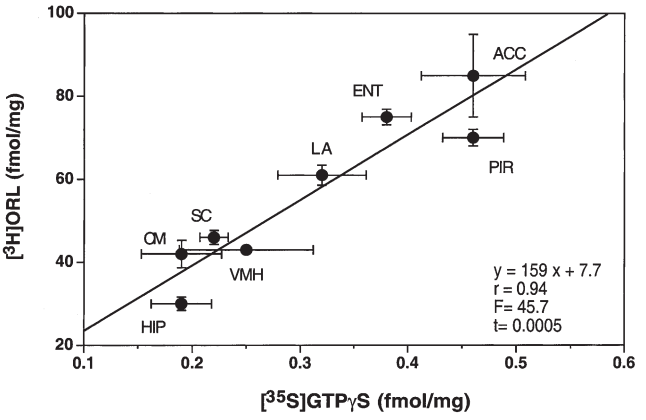

Fig. 1. Relationship between the levels of [^{3}H]N/OFQ and N/OFQ-stimulated [^{35}S]GTPγS binding in the eight forebrain regions shown in Table 1. Note the high correlation between the levels of ORL-1 receptors and N/OFQ-activated G-proteins (r=0.94).

in providing data regarding the relative levels of [^{3}H]N/OFQ and N/OFQ-stimulated [^{35}S]GTPγS binding in the ACC as compared with other regions. Furthermore, differential areal and laminar distributions of [^{3}H]N/OFQ and N/OFQ-stimulated [^{35}S]GTPγS binding in the cortex may reflect functional characteristics of the ORL-1 receptor system.

The levels of [^{3}H]N/OFQ and N/OFQ-stimulated [^{35}S]GTPγS binding varied throughout the cingulate cortex, with the highest levels in areas 24, 25 and 32, and lower levels in posterior area 29 (Fig. 2a–d). In ACC, moderate levels of ORL-1 receptors and activated G-proteins were seen in layers I–III, and both peaked in layers V and VI (Fig. 2a,b). N/OFQ binding and stimulation were generally higher in area 24a, and lower in area 24b. Indeed, the laminar preference of N/OFQ binding/stimulation for layer V in adjacent sensorimotor areas is first observed in area 24b.

There were a number of laminar variations in N/OFQ binding and G-protein activity in posterior cingulate cortex (PCC; Fig. 2c,d). Area 29c had the highest overall level of [^{3}H]N/OFQ binding and it was relatively homogenous among layers, whereas N/OFQ-stimulated [^{35}S]GTPγS binding was highest in layers I and IV and lower in layers II–III, V and VI. Area 29d, in contrast, had high levels of [^{3}H]N/OFQ binding in layers I–IV and less in layers V and VI, whereas N/OFQ-stimulated [^{35}S]GTPγS binding was moderate in layer III and low in all other layers. Caudal to the splenium of the corpus callosum, areas 29a and 29b had moderate levels of receptor binding in most layers, while N/OFQ-activated G-proteins were high in layers I, Va, and VIb. Thus, in PCC, the laminar distribution of ORL-1 receptor binding appears to be more diffuse whereas N/OFQ-stimulated [^{35}S]GTPγS binding has preference for layers II and IV or V.

As noted above, high levels of N/OFQ binding were found in hippocampal and parahippocampal cortices

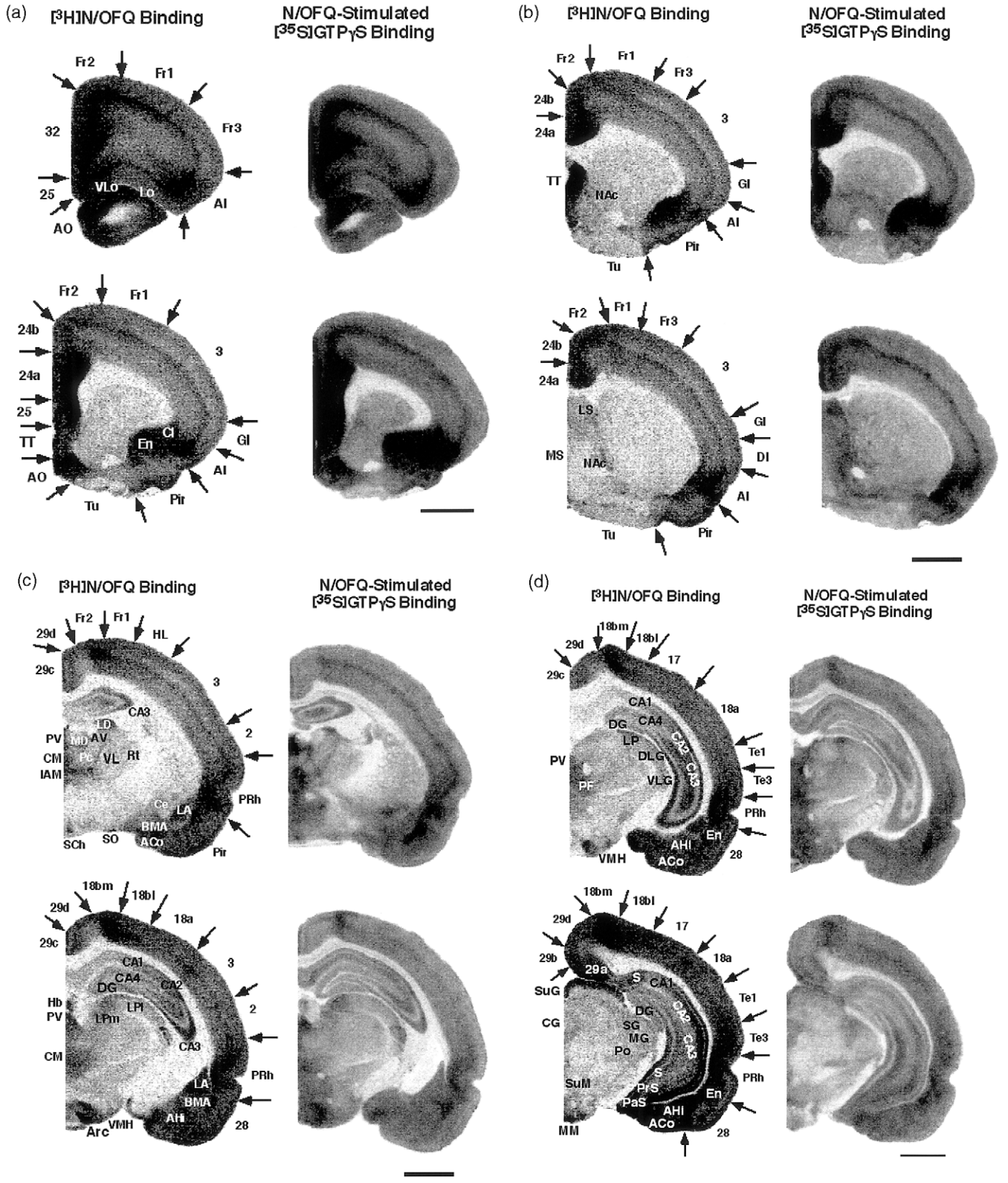

Fig. 2. a–d Autoradiograms showing [^{3}H]N/OFQ and N/OFQ-stimulated [^{35}S]GTPγS binding. The highest levels of ORL-1 receptors and activated G-proteins are seen throughout the cortex and in limbic structures. Although the relative levels of ORL-1 receptors and receptor-activated G-proteins are generally similar, there are apparent mismatches between these levels in subnuclei of the amygdala and hypothalamus. Regions were determined by analysis of thionin-stained sections. (bar=2 mm.)

(Fig. 2c,d). In the hippocampal formation, the greatest binding for both ORL-1 receptors and activated G-proteins was in the stratum radiatum and oriens of the CA2/3 sectors, while there was little or none in the stratum pyramidale. There was less overall binding in the CA1 and CA4 sectors, the subiculum, presubiculum and parasubiculum, and very little in the dentate gyrus. Like area 24a, the agranular insula had a very high level of both markers extending through the full cortical depth (Fig. 2a,b). The dysgranular insula had a high level of binding in layers I–IV and VI, while the granular insula showed greater differentiation of binding with more binding in layers II–III and V, less in layer VI and least in layers IV and Vb. Piriform, perirhinal and entorhinal cortices, the endopiriform nucleus, and claustrum all had high and relatively homogenous binding. Only at the junction of the piriform and endopiriform areas and layer III of entorhinal cortex was there a decrease in binding for both markers. It should also be noted that there was not an exact match between ORL-1 receptor binding and activated G-proteins in layers I and II of some cortices. In entorhinal and perirhinal cortices, for example, there was high ORL-1 receptor binding, while in these same layers there was low N/OFQ-stimulated [^{35}S]GTPγS binding.

Frontal cortex expressed a wide range of laminar binding distributions (Fig. 2a–c). FR2 adjacent to area 24b had the highest level of binding that was mainly confined to the superficial layers. Although a similar pattern was seen in FR1, both markers had a clear demarcation of layer Va binding, and in FR3 most superficial binding was low and the layer Va component stood out as a single layer. Finally, orbital cortex had a similar progression in the differentiation of binding observed in dorsal areas with Vlo having high and relatively homogeneous binding, but this was reduced in superficial layers and layer VI of Lo so that there was a distinct layer Va binding.

Binding in parietal and occipital sensory cortices was found primarily in layers I, II and Va. Layer IV was noticeably free of binding for both markers in areas 3 and 2, while area 2 had an additional component of binding in layer VI that seemed to be an extension of binding in the perirhinal cortex. The laminar differentiation of the ORL-1 system was particularly dramatic in the visual cortex (Fig. 2c,d). The medial division of area 18b (area 18bm) had the highest overall activity for both ORL-1 receptors and activated G-proteins and there was almost no laminar preference. Area 18bl had less binding in layers III and IV, and there was less overall binding in areas 17 and 18a with layer Va standing out with the highest levels. As noted previously, a mismatch between these two markers appears to occur in layers I–III, where [^{3}H]N/OFQ binding appeared higher than N/OFQ-stimulated [^{35}S]GTPγS binding. Finally, area Te3 had a high overall level of binding with a reduction only in layer II and areas Te3 and Te1 had progressively differentiating binding with most in layer Va, although laminar distinctions in binding were weakest in these auditory areas.

In addition to the cortex, specific regions of the amygdala, thalamus and hypothalamus contained high levels of [^{3}H]N/OFQ and N/OFQ-stimulated [^{35}S]GTPγS binding (Fig. 2c,d). In the amygdala, the highest levels were found in the lateral and basomedial nuclei, the amygdalohippocampal area, and the anterior cortical nucleus. Moderate binding was seen in the central nucleus of the amygdala. Although discrete nuclei were identified for [^{3}H]N/OFQ binding, N/OFQ-stimulated G-protein activity was quite diffuse throughout the amygdala. The midline and intralaminar thalamic nuclei had high levels of binding for both markers, whereas the anterior nucleus and many of the lateral and ventral nuclei had low levels of binding. The former nuclei include the paraventricular, interanteromedial, central medial, rhomboid, reuniens, paracentral, and parafascicular nuclei. High levels of [^{3}H]N/OFQ binding were also seen in the laterodorsal nucleus, and there was a moderate level of [^{3}H]N/OFQ binding in the ventrolateral, lateral geniculate, and suprageniculate nuclei. In the hypothalamus, the highest levels of binding were found in the suprachiasmatic, supraoptic, arcuate and ventromedial nuclei.

Several areas contained very low levels of ORL-1 receptors and G-protein activity. There was light to moderate N/OFQ binding and G-protein activity in the olfactory tubercle and nucleus accumbens shell (Fig. 2a,b). There were conspicuously low levels of both markers in the caudate-putamen, core region of the nucleus accumbens, and globus pallidus (Fig. 2a,b).

Despite the general concordance between the localization and density of [^{3}H]N/OFQ and N/OFQ-stimulated [^{35}S]GTPγS binding, there were several regions in which there was a higher level of G-protein stimulation than receptor binding (Fig. 2a–c). These regions included the lateral and medial septum, anterior hypothalamus, dorsomedial hypothalamus, posterior hypothalamus, supramammilary nucleus, periaqueductal gray and suprageniculate nucleus.

3.2. Binding in the ACC following excitotoxin and deafferentation lesions

The cellular localization of ORL-1 receptors in ACC was investigated using injections of ibotenic acid or surgical deafferentation, followed by in vitro [^{3}H]N/OFQ and N/OFQ-stimulated [^{35}S]GTPγS autoradiography. Control binding was measured in the contralateral cingulate cortex in undercut ablated animals because no difference in binding was found between these hemispheres and the unablated controls. Four brains with unilateral ibotenic acid lesions confined to ACC and were used to evaluate [^{3}H]N/OFQ and N/OFQ-stimulated [^{35}S]GTPγS binding (Fig. 3). Ibotenic acid almost completely elimin-

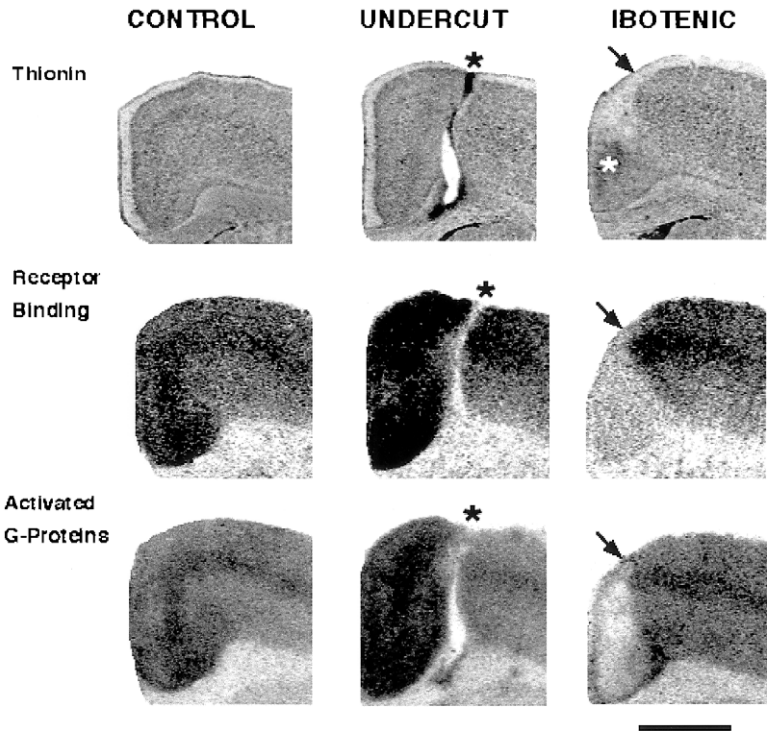

Fig. 3. Autoradiograms showing anterior cingulate cortex in control, ibotenic acid lesion and undercut lesion brains. Ibotenic acid ablation visibly reduced both ORL-1 receptor and N/OFQ-stimulated G-protein binding. In contrast, a visible increase in ORL-1 receptor binding is apparent in brains from deafferented animals. Autoradiograms of [^{3}H]N/OFQ and N/OFQ-stimulated [^{35}S]GTPγS binding were analyzed densitometrically to quantify these findings (data presented in Table 2). Thionin-stained sections were used to confirm lesion placement. The asterisk indicates lesion sites, and the point of ibotenic acid injection is marked by the arrow (bar=1.5 mm).

Table 2
Receptor binding and N/OFQ-activated G-proteins in anterior cingulate cortex

	AREA 24a		AREA 24b	
	[^{3}H]N/OFQ	Net N/OFQ-Stim [^{35}S]GTPγS	[^{3}H]N/OFQ	Net N/OFQ-Stim [^{35}S]GTPγS
Control	91.12±8.68	0.362±0.060	78.53±4.79	0.409±0.054
Undercut	134.23±13.26∗	0.442±0.056	108.03±6.59∗∗	0.432±0.049
Ibotenic	18.85±1.77∗∗	−0.009±0.028∗∗	20.38±2.36∗∗	−0.022±0.006∗∗

[^{3}H]N/OFQ and N/OFQ-stimulated [^{35}S]GTPγS binding in the anterior cingulate cortex following undercut and ibotenic acid lesions. Values are expressed in fmol/mg and are the results of analysis of triplicate sections from six control and undrcut lesion and four ibotenic lesion brains (∗ $p<0.05$; ∗∗ $p<0.005$).

ated both [^{3}H]N/OFQ receptor binding and N/OFQ-stimulated [^{35}S]GTPγS binding in ACC (Fig. 3). Densitometric analysis in layer V confirmed that [^{3}H]N/OFQ binding decreased by 79% and 74% in areas 24a and 24b, respectively (Table 2). This decrease in receptor binding was paralleled by a dramatic decrease in N/OFQ-stimulated [^{35}S]GTPγS binding (Table 2). In fact, the mean levels of N/OFQ-stimulated [^{35}S]GTPγS binding did not significantly differ from basal [^{35}S]GTPγS binding produced in the absence of agonist. In addition, a decrease in basal [^{35}S]GTPγS binding was seen following ibotenic acid lesions. Basal [^{35}S]GTPγS binding in area 24a decreased from 0.347±0.026 fmol/mg to 0.164±0.039 fmol/mg (53% decrease; p=0.005) and in area 24b basal [^{35}S]GTPγS binding decreased from 0.34±0.023 fmol/mg to 0.121±0.008 fmol/mg (64% decrease; p=0.0001).

Examination of thionin-stained sections confirmed that undercut lesions produced deafferentation of ACC (Fig. 3, top). Visual inspection of sections showed a discernible increase in [^{3}H]N/OFQ binding, but only a slight increase in N/OFQ-stimulated [^{35}S]GTPγS binding (Fig. 3). Densitometric analysis confirmed this increase in [^{3}H]N/OFQ binding; the levels of ORL-1 receptors in

layer V increased by 47% and 38% in areas 24a and 24b, respectively (Table 2). Although N/OFQ-stimulated [^{35}S]GTPγS binding increased by 22% in area 24a and 6% in area 24b, these values were not statistically significantly different from control values (Table 2). No significant changes in basal [^{35}S]GTPγS binding were found in area 24a (0.347±0.026 fmol/mg vs. 0.372±0.038 fmol/mg) or area 24b (0.34±0.023 fmol/mg vs. 0.392±0.034 fmol/mg). The lesion data are summarized graphically in Fig. 4, where [^{3}H]N/OFQ and N/OFQ-stimulated [^{35}S]GTPγS binding in ibotenic acid and undercut ablated animals is expressed as percent of control animals.

4. Discussion

High levels of [^{3}H]N/OFQ and N/OFQ-stimulated [^{35}S]GTPγS binding were found throughout the cortex, amygdala, hippocampus, thalamus and hypothalamus. Particularly high levels of ORL-1 receptors and receptor-activated G-proteins were found in the ACC, where binding peaked in layers V and VI. The cellular localization of ORL-1 receptors in ACC was investigated using a lesion strategy: excitotoxin lesions to destroy neurons or deafferentation to remove afferent axons. Post-lesion localization indicates that ORL-1 receptors in layer V of the ACC are somatodendritic because they are eliminated after excitotoxin lesion and increased following deafferentation.

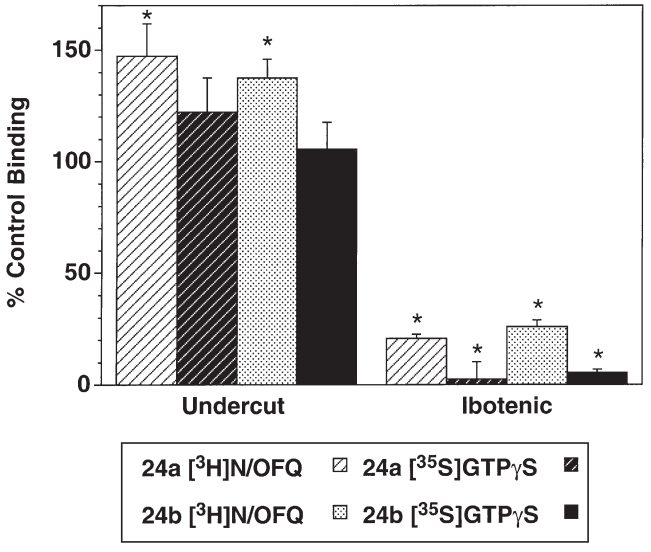

Fig. 4. Summary graph of the effects of ibotenic acid and undercut lesions on [^{3}H]N/OFQ binding and N/OFQ-stimulated [^{35}S]GTPγS binding expressed as percent of control binding in area 24a and 24b. Ibotenic acid ablation produced a loss of ORL-1 receptor binding and G-protein activation, whereas deafferentation increased ORL-1 receptor binding. These data indicate that ORL-1 receptors are localized on somatodendritic elements in layer V of the ACC (∗$p<0.005$; †$p<0.05$).

This study is the first to correlate ORL-1 receptor binding with ORL-1-activated G-proteins. Interestingly, the data suggest there may be regions of mismatch between the relative levels of receptors and activated G-proteins. The most apparent mismatch between [^{3}H]N/OFQ and N/OFQ-stimulated [^{35}S]GTPγS binding was found in specific regions of the hypothalamus (i.e. anterior, dorsomedial, posterior and supramammillary nuclei), and amygdala. For example, the central and medial nuclei of the amygdala exhibit higher levels of ORL-1-activated G-proteins compared to ORL-1 receptors, indicating that receptor number does not completely correlate with functional activity. These are also areas in which relatively high levels of basal [^{35}S]GTPγS binding are found, indicating that receptors in these areas may be more active compared to other regions. Since the [^{35}S]GTPγS assay does not differentiate between different subtypes of G-proteins, this may reflect differences in affinities of the Gα subtypes for [^{35}S]GTPγS. Another consideration is that N/OFQ is an agonist, and thus preferentially recognizes the high affinity state of the receptor. There may be low affinity ORL-1 receptors in these regions that were not detected using this method, thus underestimating the levels of ORL-1 binding sites in some regions.

The present results show a similar relative regional relationship for [^{3}H]N/OFQ binding (i.e. cerebral cortex>amygdala>hippocampus) as a previous study in mouse forebrain (Florin et al., 1997). However, the laminar distribution of ORL-1 receptors in cingulate cortex differs between the two reports. The present data showed a clear peak in binding in layers V and VI of the ACC, whereas Florin et al. report “diffuse labeling” in the cingulate cortex. More recent reports have described the distribution of ^{125}I-[^{14}Tyr]-N/OFQ binding in rat brain (Neal et al., 1999). The overall regional distribution described by the two studies is similar, although the regional comparison provided in Fig. 1 of this study seems to differ somewhat from regional data provided in Table 2 by Neal et al. For example, measurements in the ventromedial hypothalamus and superior colliculus were relatively lower in this study than reported by Neal et al., whereas those in the lateral amygdala and entorhinal cortex were relatively higher. This probably reflects (1) differences in the specificity of analysis (i.e. our cortical measurements were confined to the layers with highest binding density) and (2) difficulty in accurately comparing the qualitative scheme used by Neal et al with data presented in Table 1. Overall, the distribution of ORL-1 receptors demonstrated by [^{3}H]N/OFQ and ^{125}I-[^{14}Tyr]-N/OFQ binding are similar. A notable exception is the central and basomedial nuclei of the amygdala, which contained moderate levels of [^{3}H]N/OFQ binding and low levels of ^{125}I-[^{14}Tyr]-N/OFQ binding. Other forebrain areas were reported to have moderate levels of ^{125}I-[^{14}Tyr]-N/OFQ binding, such as lateral septum,

olfactory tubercle and nucleus accumbens shell, but showed low levels of [^{3}H]N/OFQ binding. However, comparison of figures showing ^{125}I-[^{14}Tyr]-N/OFQ versus [^{3}H]N/OFQ binding in brain sections reveal similar levels of binding, indicating that different criteria were used in the two studies. Perhaps the most obvious discrepancy between the two studies is the laminar distribution of ORL-1 receptors in the cortex. For example, [^{3}H]N/OFQ binding was more homogeneous in entorhinal, piriform and posterior cingulate cortices than ^{125}I-[^{14}Tyr]-N/OFQ binding. [^{3}H]N/OFQ binding also exhibited a more complex laminar distribution in frontal cortex (FR1, FR2, FR3) than ^{125}I-[^{14}Tyr]-N/OFQ.

Comparison of the present results with the localization of N/OFQ peptide by Neal et al. (1999a) reveals a general correspondence between the gross regional distribution of ORL-1 binding sites, ORL-1-activated G-proteins and N/OFQ immunoreactivity (-ir) in the forebrain. However, in several regions there is an apparent mismatch between the distribution of ORL-1 receptors in this study and N/OFQ-ir described by Neal et al. Examination of the ACC reveals a mismatch in the relative levels of N/OFQ-ir versus ORL-1 receptors. The ACC was one of the regions with the highest levels of ORL-1 receptors (see Table 1), but Neal et al. reported that the cingulate cortex stained only lightly for N/OFQ-ir cell bodies and fibers/terminals. Perhaps the most obvious mismatch between ORL-1 receptors and N/OFQ-ir was found in the amygdala and hypothalamus, regions in which mu opioid receptor and opioid peptide levels also differ (Herkenham, 1987). For example, high levels of ORL-1 receptors are found in the anterior cortical, lateral and basomedial nuclei of the amygdala, yet these areas contain low amounts of N/OFQ-ir. This finding suggests the possibility that there may be other endogenous ligands for this receptor. Conversely, very high levels of N/OFQ-ir are found in the central and medial nuclei, whereas ORL-1 receptor binding is low to moderate, which may be due to the presence of internalized receptors, as discussed below.

An interesting comparison can be made regarding the cortical laminar distribution of ORL-1 receptors, G-protein activity and N/OFQ-ir. In many cortical regions, ORL-1 receptor binding was appreciably higher than receptor-activated G-proteins or N/OFQ-ir in layers I–III. Previous studies on cannabinoid receptors have shown differences in the relative efficiency of receptors between different brain regions (Breivogel et al., 1997) and cortical laminae (Sim-Selley et al., 2002). Results from the present study indicate that similar differences in receptor efficiency occur in the ORL-1 system. It is also possible that ORL-1 receptors in superficial lamina act via a different type of G-protein than those identified in deeper lamina. The [^{35}S]GTPγS binding assay primarily recognizes G-proteins of the G_i/G_o family, and ORL-1 receptors have also been reported to activate $G\alpha_z$ and $G\alpha_{16}$ in cultured cell lines (Chan et al., 1998). These G-proteins have a very slow rate of GTP/GDP exchange (Casey et al., 1990) and may not have been detected under conditions favoring G_i/G_o.

Regions were also identified in which N/OFQ-ir is found, but very little ORL-1 binding or G-protein activity is seen. These areas are primarily located in the striatum and basal ganglia, and include caudate-putamen, globus pallidus and nucleus accumbens core. Some studies have suggested that there may be heterogeneity of ORL-1 receptors (Mathis et al., 1997), possibly via the generation of splice variants of the receptor (Wang et al., 1994). Another explanation could be that ORL-1 receptors in some regions are internalized in the native state and thus cannot bind ligand or activate G-proteins. This finding has been reported for neurotensin receptors in the substantia nigra, where a percentage of dendritic receptors are immunolabeled, but are not detectable using receptor autoradiography (Boudin et al., 1998).

One of the interesting findings of this study was that deafferentation increased the levels of [^{3}H]N/OFQ binding, but produced no change in ORL-1-activated G-proteins. Increased [^{3}H]N/OFQ binding may reflect ORL-1 receptor upregulation. This suggests that the number of high affinity ORL-1 receptors increase, as predicted from a somatodendritic receptor response to deafferentation. It is also possible that the measured increase in [^{3}H]N/OFQ binding reflects an increase in the affinity of the receptor for agonist. An unexpected result was that the increase in ORL-1 receptor binding occurred in the absence of any significant change in the level of ORL-1-activated G-proteins. This lack of correlation with the increase in [^{3}H]N/OFQ binding may be important because the correlation between ORL-1 receptors and activated G-proteins was very high ($r>0.9$) in control brains (Fig. 1), and the loss of [^{3}H]N/OFQ sites following ibotenic acid lesions was accompanied by a similar loss in N/OFQ-stimulated [^{35}S]GTPγS binding (Table 2). There are several possible explanations for the difference in this relationship following deafferentation. Neither [^{35}S]GTPγS nor [^{3}H]N/OFQ was used at a saturating concentration (L.J. Sim-Selley and S.R. Childers, unpublished observations), so none of these experiments produced binding at the B_{max} level. Also, tissue sections are 20 μm thick, so [^{35}S]GTPγS may not penetrate beyond the most superficial portion of the section. Another explanation is that upregulated ORL-1 receptors do not couple to neuronal G-proteins with the same efficiency as normal receptors, implying that the functional consequences of neuronal deafferentation cannot be predicted from receptor binding alone.

Homology between opioid and ORL-1 receptors has generated interest in similarities/differences between these two receptors. Vogt et al. (1995) have described the localization of mu and delta opioid receptors in the

rat ACC. The laminar distribution of ORL-1 receptors in the ACC parallels delta opioid receptors; both are found in all layers, with a peak in binding in layers V and VI. Another similarity is that both ORL-1 and delta receptors in ACC are localized on somatodendritic elements. An interesting difference between delta and ORL-1 receptors is that ORL-1 receptors increased following deafferentation, whereas delta receptors did not (Vogt et al., 1995), suggesting differences in regulation of these receptors in ACC. Mu opioid receptors are found in all layers of ACC, with the highest density in layer I (Vogt et al., 1995). Mu receptors exhibit both axonal and somatodendritic localization, indicating that they modulate both inputs to ACC via receptors in superficial layers and ACC output via projection neurons in deep layers. This distribution suggests a fundamentally different mode of action for ORL-1 versus mu receptors in ACC, and provides multiple schemes by which mu and ORL-1 receptors could interact in this region.

Localization of ORL-1 receptors to layers V and VI of ACC suggests that these receptors influence the activity of ACC projection neurons. This is supported by the apparent somatodendritic localization of ORL-1 receptors. The presence of ORL-1 receptors on ACC projection neurons would allow modulation of neuronal activity in terminal field regions. Neurons in ACC layers V and VI project to the thalamus and layer V neurons project to the PAG (Vogt, 1993). This pathway is of potential interest given the hyperalgesic effects of i.c.v. N/OFQ and its antagonism of opioid-mediated analgesia (Meunier et al., 1995; Reinscheid et al., 1995; Grisel et al., 1996; Mogil et al., 1996; Tian et al., 1997).

In summary, ORL-1 receptors and activated G-proteins are most dense in layers V and VI of ACC and exhibit somatodendritic localization in layer V of area 24. Although the levels of ORL-1 receptors and activated G-proteins correlate in ACC, other forebrain regions and cortical layers show a mismatch between these two receptor measures. Thus, there may be differences in ORL-1 receptor efficiency between different brain areas. Furthermore, deafferentation of the ACC produced an increase in ORL-1 receptors, without a corresponding change in G-protein activation. This result illustrates the importance of examining measures of both receptor number and function, and indicates that factors other than receptor number influence ORL-1-mediated G-protein activity.

Acknowledgements

This work was supported by PHS grants DA 00287 (LJS) and DA 02904 (SRC) from NIDA and by Cingulum NeuroSciences Institute (BAV). The authors thank Ruoyu Xiao for technical assistance.

References

Anton, B., Fein, J., To, T., Li, X., Silberstein, L., Evans, C.J., 1996. Immunohistochemical localization of ORL-1 in the central nervous system of the rat. Journal of Comparative Neurology 368, 229–251.

Boudin, H., Pelaprat, D., Rostene, W., Pickel, V.M., Beaudet, A., 1998. Correlative ultrastructural distribution of neurotensin receptor proteins and binding sites in the rat substantia nigra. Journal of Neuroscience 15, 8473–8484.

Breivogel, C.S., Sim, L.J., Childers, S.R., 1997. Regional differences in cannabinoid receptor/G-protein coupling in rat brain. Journal of Pharmacology and Experimental Therapeutics 282, 1632–1642.

Bunzow, J.R., Saez, C., Mortrud, M., Bouvier, C., Williams, J.T., Low, M., Grandy, D.K., 1994. Molecular cloning and tissue distribution of a putative member of the rat opioid receptor gene family that is not a μ, δ or κ opioid receptor type. FEBS Letters 347, 284–288.

Casey, K.L., Minoshima, S., Berger, K.L., Koeppe, R.A., Morrow, T.J., Frey, K.A., 1994. Positron emission tomographic analysis of cerebral structures activated specifically by repetitive noxious stimuli. Journal of Neurophysiology 71, 802–807.

Casey, P.J., Fong, H.K.W., Simon, M.I., Gilman, A.G., 1990. G_z, a guanine nucleotide-binding with unique biochemical properties. Journal of Biological Chemistry 265, 2383–2390.

Chan, J.S.C., Yung, L.Y., Lee, J.W.M., Wu, Y.L., Pei, G., Wong, Y.H., 1998. Pertussis toxin-insensitive signaling of the ORL1 receptor: coupling to G_z and G_{16} proteins. Journal of Neurochemistry 71, 2203–2210.

Coghill, R.C., Talbot, J.D., Evans, A.C., Meyer, E., Gjedde, A., Bushnell, M.C., Duncan, G.H., 1994. Distributed processing of pain and vibration in human brain. Journal of Neuroscience 14, 4095–4108.

Evans, C.J., 1999. Corrigendum. Journal of Comparative Neurology 412, 708.

Florin, S., Leroux-Nicollet, I., Meunier, J.C., Costentin, J., 1997. Autoradiographic localization of [^{3}H]nociceptin binding sites from the telencephalic to mesencephalic regions of the mouse brain. Neuroscience Letters 230, 33–36.

Fukuda, K., Kato, S., Mori, K., Nishi, M., Takeshima, H., Iwabe, N., Miyata, T., Houtani, T., Sugimoto, T., 1994. cDNA and regional distribution of a novel member of the opioid receptor family. FEBS Letters 343, 42–46.

Grisel, J.E., Mogil, J.S., Belknap, J.K., Grandy, D.K., 1996. Orphanin FQ acts as a supraspinal, but not a spinal, anti-opioid peptide. NeuroReport 7, 2125–2129.

Hao, J.X., Xu, I.S., Wiesenfeld-Hallin, Z., Xu, X.J., 1998. Anti-hyperalgesic and anti-allodynic effects of intrathecal nociceptin/orphanain FQ in rats after spinal cord injury and inflammation. Pain 76, 385–393.

Herkenham, M., 1987. Mismatches between neurotransmitter and receptor localizations in brain: observations and implications. Neuroscience 23, 1–38.

Jones, A.K.P., Brown, W.D., Friston, K.J., Qi, L.Y., Frackowiak, R.S.J., 1991. Cortical and subcortical localization of response to pain in man using positron emission tomography. Proceedings of the Royal Society of London, Biology 244, 39–44.

King, M.A., Rossi, G.C., Chang, A.H., Williams, L., Pasternak, G.W., 1997. Spinal analgesic activity of orphanin FQ/nociceptin and its fragments. Neuroscience Letters 223, 113–116.

Knoflach, F., Reinscheid, R.K., Civelli, O., Kemp, J.A., 1996. Modulation of voltage-gated calcium channels by orphanin FQ in freshly dissociated hippocampal neurons. Journal of Neuroscience 16, 6657–6664.

Lachowicz, J.E., Shen, Y., Monsma, F.J., Sibley, D.R., 1995. Molecular cloning of a novel G-protein-coupled receptor related to the opiate receptor family. Journal of Neurochemistry 64, 34–40.

Mathis, J.P., Ryan-Moro, J., Chang, A., Hom, J.S.H., Scheinberg, D.A., Pasternak, G.W., 1997. Biochemical evidence for orphanin

FQ/nociceptin recepotr heterogeneity in mouse brain. Biochemical and Biophysical Research Communications 230, 462–465.

Matthes, H., Seward, E.P., Kieffer, B., North, R.A., 1996. Functional selectivity of orphanin FQ for its receptor coexpressed with potassium channel subunits in *Xenopus laevis* oocytes. Molecular Pharmacology 50, 447–450.

Meunier, J.-C., Mollereau, C., Toll, L., Suaudeau, C., Moisand, C., Alvinerie, P., Butour, J.-L., Guillemot, J.-C., Ferrara, P., Monsarrat, B., et al. 1995. Isolation and structure of the endogenous agonist of opioid receptor-like ORL1 receptor. Nature 377, 532–535.

Meunier, J.C., 1997. Nociceptin/orphanin FQ and the opioid receptor-like ORL1 receptor. European Journal of Pharmacology 340, 1–15.

Mogil, J.S., Grisel, J.E., Zhangs, G., Belknap, J.K., Grandy, D.K., 1996. Functional antagonism of μ-, δ- and κ-opioid antinociception by orphanin FQ. Neuroscience Letters 214, 131–134.

Mollereau, C., Parmentier, M., Mailleaux, P., Butour, J.-L., Moisand, C., Chalon, P., Caput, D., Vassart, G., Meunier, J.-C., 1994. ORL1, a novel member of the opioid receptor family. FEBS Letters 341, 33–38.

Neal, C.R., Mansour, A., Reinscheid, R., Nothnacker, H.-P., Civelli, O., Watson, S.J., 1999a. Localization of orphanin FQ (nociceptin) peptide and messenger RNA in the central nervous system of the rat. Journal of Comparative Neurology 406, 503–547.

Neal, C.R., Mansour, A., Reinscheid, R., Nothnacker, H.P., Civelli, O., Akil, H., Watson, S.J., 1999b. Opioid receptor-like (ORL-1) receptor distribution in the rat central nervous system: comparison of ORL1 receptor mRNA expression with ^{125}I-[^{14}Tyr]-orphanin FQ binding. Journal of Comparative Neurology 412, 563–605.

Paxinos, G., Watson, C., 1986. The Rat Brain in Stereotaxic Coordinates. San Diego, CA, Academic Press.

Reinscheid, R.K., Nothacker, H.-P., Bourson, A., Ardati, A., Henningsen, R.A., Bunzow, J.R., Grandy, D.K., Langen, H., Monsma, F.J., Civelli, O., 1995. Orphanin FQ: a neuropeptide that activates an opioid-like G protein-coupled receptor. Science 270, 792–794.

Rosen, A., Lundeberg, T., Bytner, B., Nylander, I., 2000. Central changes in nociceptin, dynorphin B and Met–enkephalin–Arg–Phe in different models of nociception. Brain Research 857, 212–218.

Sikes, R.W., Vogt, B.A., 1992. Nociceptive neurons in area 24b of rabbit cingulate cortex. Journal of Neurophysiology 68, 1720–1732.

Sim, L.J., Xiao, R., Childers, S.R., 1996. Identification of opioid receptor-like (ORL1) peptide-stimulated [^{35}S]GTPγS binding in rat brain. NeuroReport 7, 729–733.

Sim-Selley, L.J., Vogt, L.J., Vogt, B.A., Childers, S.R., 2002. Cellular localization of cannabinoid receptors and activated G-proteins in rat anterior cingulate cortex. Life Science 71, 2217–2226.

Tian, J.H., Xu, W., Fang, Y., Mogil, J.S., Grisel, J.E., Grandy, D.K., Han, J.S., 1997. Bidirectional modulatory effect of orphanin FQ on morphine-induced analgesia: antagonism in brain and potentiation in spinal cord of the rat. British Journal of Pharmacology 120, 676–680.

Vaughn, C.W., Christie, M.J., 1996. Increase by the ORL1 receptor (opioid receptor-like1) ligand, nociceptin, of inwardly rectifying K conductance in dorsal raphe nucleus neurones. British Journal of Pharmacology 117, 1609–1611.

Vogt, B.A., 1993. Structural organization of cingulate cortex: areas, neurons, and somatodendritic transmitter receptors. In: Vogt, B.A., Gabriel, M. (Eds.), Neurobiology of Cingulate Cortex and Limbic Thalamus. Birkhauser, Boston.

Vogt, B.A., Derbyshire, S., Jones, A.K., 1996. Pain processing in four regions of human cingulate cortex localized with co-registered PET and MR imaging. European Journal of Neuroscience 8, 1461–1473.

Vogt, B.A., Peters, A., 1981. Form and distribution of neurons in rat cingulate cortex: areas 32, 24, and 29. Journal of Comparative Neurology 195, 603–625.

Vogt, B.A., Wiley, R.G., Jensen, E.L., 1995. Localization of mu and delta opioid receptors to anterior cingulate afferents and projection neurons and input/output model of mu regulation. Experimental Neurology 135, 83–92.

Vogt, L.J., Vogt, B.A., Sikes, R.W., 1992. Limbic thalamus in rabbit: architecture, projections to cingulate cortex and distribution of muscarinic acetylcholine, GABAA, and opioid receptors. Journal of Comparative Neurology 319, 205–217.

Wang, J.B., Johnson, P.S., Imai, Y., Persico, A.M., Ozenberger, B.A., Eppler, C.M., Uhl, G.R., 1994. cDNA cloning of an orphan opiate receptor gene family member and its splice variant. FEBS Letters 348, 75–79.

Wick, M.J., Minnerath, S.R., Lin, X., Elde, R., Law, P.Y., Loh, H.H., 1994. Isolation of a novel cDNA encoding a putative membrane receptor with high homology to the cloned μ, δ and κ opioid receptors. Molecular Brain Research 27, 37–44.

Zhu, C.B., Cao, X.D., Xu, S.F., Wu, G.C., 1997. Orphanin FQ potentiates formalin-induced pain behavior and antagonizes morphine analgesia in rats. Neuroscience Letters 1997, 37–40.

Zilles, K., 1985. The Cortex of the Rat: A Stereotaxic Atlas. Springer-Verlag, Berlin/Heidelberg/New York.